Available online at www.sciencedirect.com
SCIENCE DIRECT®
Journal of Sound and Vibration 271 (2004) 209–225
JOURNAL OF SOUND AND VIBRATION
www.elsevier.com/locate/jsvi

Modelling of vibro-impact penetration of self-exciting percussive-rotary drill bit

A.D. Batako*, V.I. Babitsky, N.A. Halliwell

Wolfson School of Mechanical and Manufacturing Engineering, Loughborough University, Loughborough, Leicestershire LE11 3TU, UK

Received 17 September 2002; accepted 24 February 2003

Abstract

The penetration of a drilling tool into a hard medium under periodic impact action is analyzed and the simulation model presented. This is further development of previously investigated model of a self-excited percussive-rotary drilling system. The system used the stick–slip phenomenon to generate an impact action superimposed on the drilling process. A phenomenological visco-elasto-plastic model of the media is used and the system response is studied numerically, first as a forced vibration and second as a result of a self-excited vibro-impact process. Relief of the main drive has been obtained and an increase in the rate of penetration is observed with increased impact intensity and hardening of the medium. Results of the preliminary drilling experiment with superimposed dynamic action have shown an improvement in the rate of penetration.

1. Introduction

Improvement is constantly sought when drilling in order to increase the rate of penetration (ROP), the time span between maintenance services, the life of the drilling system and to reduce the overall cost of the drilling process. Current drilling trends tend to increase the ROP by balancing the speed of rotation and the weight on the bit. This often leads to a failure of the drill string, which undergoes complex loading. The load is exerted in such a way that the upper part of the drill string is in extension and the lower part is in compression. The top drive rotates the drill pipe with the bit, which cuts the rock formation at the bottom. Consequently, the entire drill

*Corresponding author. Tel.: +44-1512312126; fax: +44-1512312590.
E-mail address: a.d.batako@livjm.ac.uk (A.D. Batako).

0022-460X/$ - see front matter © 2003 Elsevier Ltd. All rights reserved.
doi:10.1016/S0022-460X(03)00642-4

string works in torsion and experiences axial and torsional vibration. To control the parameters of the drilling process (actual speed of rotation, weight on bit, and torque on bit), complex techniques are used in order to detect and monitor the whirl, stick–slip vibration and the forces and stresses in the drill string. This increases the cost of operation with a reduced outcome [1].

In Ref. [2] published previously, the authors presented a self-oscillatory system for percussive-rotary drilling, which relieves the drill string of torsional vibration and the main drive from overload. In this paper, the authors investigate the relief of the thrust due to the impacts generated by the mechanism. The model presented takes the properties of the media being drilled into consideration in order to estimate the ROP.

2. Early vibro-impact penetration concepts

Vibro-impact mechanisms have been studied and widely used in engineering in the former Soviet Union since the post-war period. The major research work was concerned with finding adequate parameters (maximum impact force) for the development of new machines and intensification of the penetration due to the use of different mechanisms of excitation of vibration and impacts. Basic models of machines were developed including the interaction with the medium during the penetration [3–8]. This gradually brought about the formation of the general theory of vibro-impact systems (see Ref. [9] and bibliography).

Early models of vibro-impact penetration of a tool into a medium were introduced by Tsaplin [3], who assumed an instantaneous impact force and the velocities before and after impact were related through a restitution coefficient. Later, Tsaplin introduced a depth dependency by gradually increasing the mass of the driven element as the pile moves into the medium. The vibration and vibro-impact methods of penetration into different media owed their practical widespread to the works of Barkan [4], Savinov and Luskin [5] and Tseitlin et al. [8]. The initial theoretical analysis of the vibro-penetration process was made by Neimark [10] and Blekhman [11,12].

Two models of the indenter–footing resistance were mainly used to reflect the primary experimental data. In the purely plastic model, the resistance [5,7] was presented as weightless plug held in the borehole by the permanent force. The advance of the plug is possible when the sum of the applied forces exceeds the resistance force. Under these circumstances the plug followed to the movement of the indenter.

An elasto-plastic model, known as Prandtl model, took into consideration the elasticity of the medium by adding an ideal spring between the indenter and plug [5,7]. In this model, the movement of the plug is only possible when the elastic force of the spring exceeds the resistance of the medium. More complex rheological models of the medium were also used (see for example Refs. [5,7,13–16] etc.).

In percussive-rotary drilling the tool moves into the medium by an impact–scratching action and inherently removes off cuttings. This permits use of a simplified model to estimate the ROP due to impact. The model below takes into consideration the frontal resistance of the medium as an elasto-plastic process and viscous dissipation during the vibration of the bit.

3. The percussive-rotary drilling model

The dynamic response of the model in Fig. 1 has been studied in Ref. [1]. This is a self-excited and self-synchronising system where, due to the dry friction, the bit displays a stick–slip motion. The drive 1 represents the entire drilling system with a total mass greatly exceeding the mass of the drill bit. Therefore, it is considered that the drive 1 moves with a velocity v, which is not affected by the activity of the bit. The purpose of it is to decouple the vibration of the bit from the drill string. This is achieved with the help of a special mechanism, which is represented by the springs 3 and 6, the dashpot and the lever 5. There exist different techniques of implementing this decoupling mechanism. Hydraulic actuators, cams, system of levers, specially designed springs or mechanically reciprocating devices could be used for this purpose.

The dry friction at the interface induces a stick–slip motion, which excites the striker 4 to impart blows onto the bit 2. The periodic vibro-impact motion of the system was obtained numerically where the striker 4 impacts on the bit and both the striker and the bit synchronise their periodic motions. The frequency of synchronised motion was estimated as $\sqrt{(k_1 + k_2)/m_1}$, [1].

3.1. Description of the model of impact penetration

Fig. 2 illustrates schematically the model of the vibro-impact penetration into a medium with visco-elasto-plastic features. This model is built upon considerations in Refs. [6,13] of the rheological behaviour of materials under vibration and impact loading. The model consists of a spring 9, which is mounted in series with a dry friction element (plug) 10. A viscous element 11 is set parallel to the elasto-plastic element. The model provides a stepwise downward displacement of the bit, provided the overall forces exceed the threshold of the force D.

The model works as follows: after a blow, imparted by the striker 4 to the bit 2, the spring 9 and the dashpot 11 are deformed gradually due to the visco-elastic properties of the medium. If the overall force developed in the spring is less than the threshold force D, the medium produces visco-elastic resistance only. At this stage, the bit will oscillate about its current position of equilibrium defined by the position of the dry friction element. Whenever the force produced by the elastic element during the compression stage becomes equal or greater than the threshold force

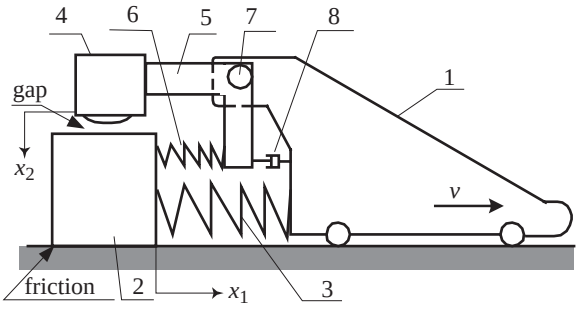

Fig. 1. Model of friction-induced self-oscillatory vibro-impact system. (1) Drive with constant velocity v; (2) bit with mass m_1; (3) main spring with stiffness k_1; (4) striker with mass m_2; (5) lever; (6) secondary spring with stiffness k_2; (7) pin; (8) dashpot with viscous coefficient c_2.

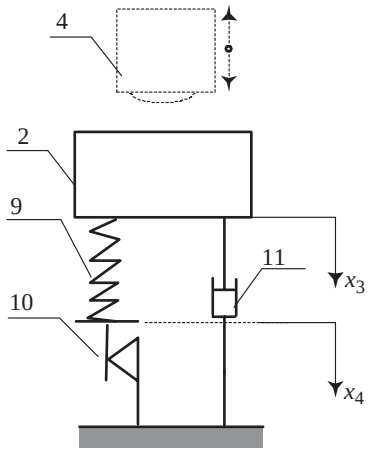

Fig. 2. Model of vibro-impact penetration into visco-elasto-plastic material. 2—bit; 4—striker; 9—spring with stiffness k_3; 10—dashpot with viscous coefficient c_3; 11—dry friction element with threshold force D.

D, the footing resistance of the medium instantly changes its nature and becomes plastic. This transformation, however, does not change the instant position and velocity of the bit. This means that the downward movement of the bit and dry friction element continues further as a coupled rigid body motion under a permanent resistance force D and the force developed by viscous element until the bit's motion is arrested. The downward displacement during this latter stage defines the ROP of the drilling bit. The dry friction element slips only in the positive direction of x_4.

After a full compression stage, which ends with a plastic slip, the bit executes a backward motion (restitution stage) due to the accumulated elastic energy in the medium corresponding to its yield point. The restitution process is carried out relative to the new position of equilibrium, shifted downward by the value of the plastic deformation. The progression of restitution flows from the visco-elastic properties of the medium and is completed when the dynamic component of the contact force between the bit and the medium vanishes.

3.2. Equations of the system motion

The equation of motion of the bit relative to its position of equilibrium $x_3 = 0$ associated with the current position x_4 of the dry friction element is defined as follows:

$$m_1\ddot{x}_3 + c_3\dot{x}_3 = -N + I\sum_{n=1}^{\infty}\delta(t - nT), \tag{1}$$

$$N = \begin{Bmatrix} k_3(x_3 - x_4) & \text{if} & 0 < k_3(x_3 - x_4) < D \\ D & \text{if} & k_3(x_3 - x_4) \geqslant D \\ 0 & \text{if} & k_3(x_3 - x_4) < 0 \end{Bmatrix}, \tag{2}$$

$$\dot{x}_4 = \left\{ \begin{array}{lll} \dot{x}_3 & \text{for} & k_3(x_3 - x_4) \geqslant D \\ 0 & \text{for} & k_3(x_3 - x_4) < D \end{array} \right\}. \tag{3}$$

In Eqs. (1) and (2), m and x_3 are the mass and the normal co-ordinate of the drill bit in condition, when the weight of the bit is equalised by the spring response (static equilibrium); $\dot{x}_3$ and $\ddot{x}_3$ are the drill bit velocity and acceleration, respectively; k_3 is a coefficient of medium elastic resistance to penetration; c_3 is the damping coefficient for the bit oscillation, x_4 is the co-ordinate of the dry friction element; $\dot{x}_4$ is its velocity and D the threshold force, at which the dry friction element slips downwards; I is the instantaneous impact impulse generated by the striker; $\delta(t)$ is the Dirac delta function and T is the period at which the impacts occur; t is the time and $n = 1, 2, 3, \ldots$. It is assumed here that, when the overall force of the spring exceeds D, the dry friction element instantly achieves the same velocity as the bit.

The analysis of the system is carried out in two steps. In the first stage, the dynamic response of the model in Fig. 2 to different prescribed force excitation will be studied and in the second stage the behaviour of the entire self-excited system will be investigated. The latter results from the interaction of the model in Fig. 1 with the model in Fig. 2.

4. Study of the response of the system

To estimate the physical parameters of the system in Fig. 2, the uniaxial compressive strength (UCS) test was carried out on samples of rock cores. Thus the threshold force D, Young's modulus and subsequently the stiffness were obtained.

The equations of motion of the system are solved numerically using the mathematical package of Matlab–Simulink. The Runge–Kutta fourth and fifth order solver with variable step is used. The Simulink toolbox enables the user to set up tags (hit crossing) at the points of specific events. At the whereabouts of these tags, Simulink increases the computing accuracy by reducing the integration step to a possible minimum, which is given as a point of tolerance. This is a helpful feature for locating events like impact or discontinuity. A sine wave excitation with increasing frequency is used to study the response of the system under a sweep test. In order to identify the resonant frequency, the sweep rate was set to 0.25, 0.5 and 1 Hz per second. To simulate impact force at a given frequency, pulses with duration of 0.002 s were used. The system was subjected firstly to a sweep sine test, secondly to periodic impact loading using pulses of variable frequency and finally under the impact force generated from the main system shown in Fig. 1.

4.1. Amplitude–frequency response with a sweep-sine test

In order to understand the response of the system, a sweep-sine test is carried out. The following short notations: $\alpha_3 = \dot{x}_3$ and $\psi_3 = x_3 - x_4$ are introduced where α_3 is the velocity of the bit relative to the medium and ψ_3 is the displacement of the bit 2 with reference to the current position of the dry friction element.

Fig. 3 depicts the amplitude–frequency response of the system presented in Fig. 2 under a sweep-sine test. The thin and thick lines are the amplitude of the displacement and the velocity of the bit, respectively. Fig. 4 shows the amplitude of the velocity of the bit and the corresponding

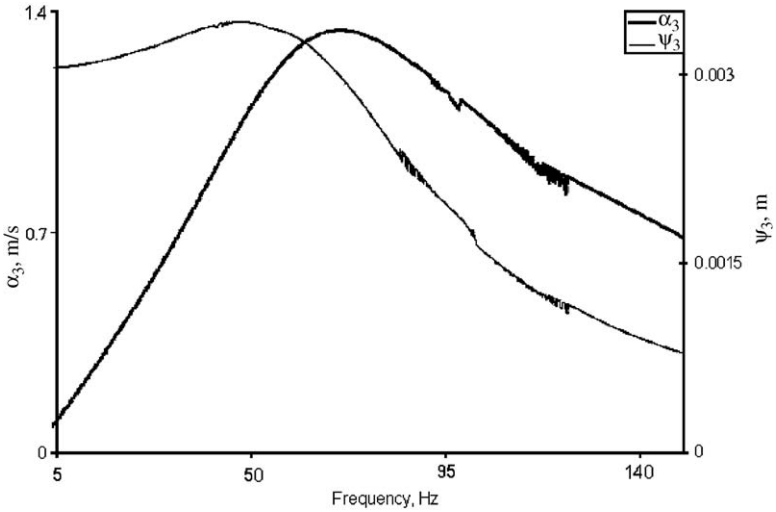

Fig. 3. Amplitude–frequency response of the system.

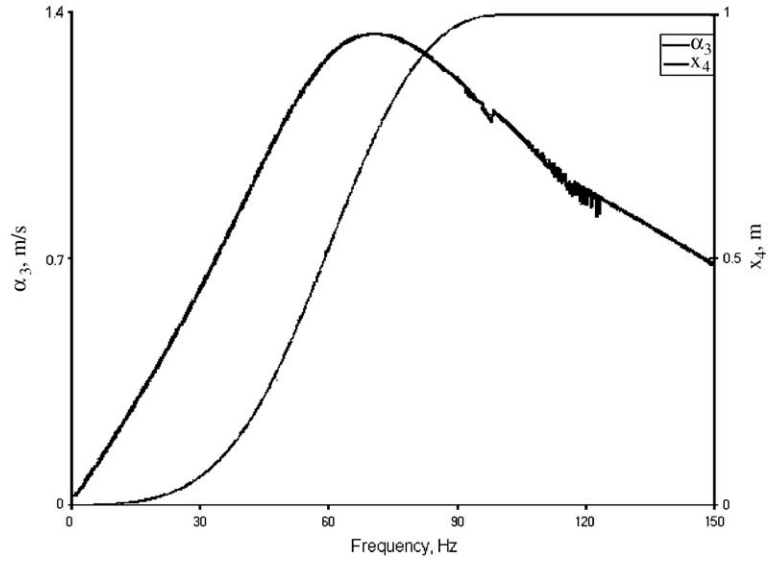

Fig. 4. Velocity of vibration and displacement of the dry friction element.

amplitude of the displacement of the dry friction element. It is seen that after the resonance, any further increase of the frequency does not produce slippage of the dry friction element. This gives an indication of the frequency range within which the vibration has positive effect on the penetration rate.

Fig. 5 displays the amplitude of the bit vibration velocity depending on the frequency for different values of the stiffness k_3 and Fig. 6 shows the respective amplitude frequency response of

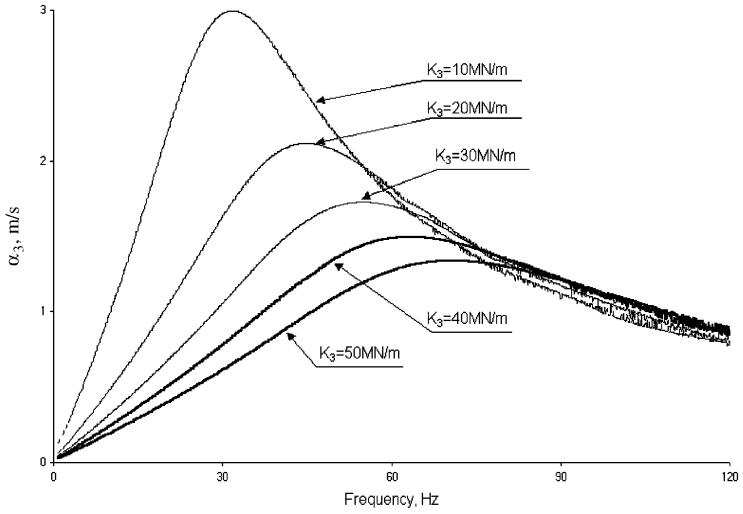

Fig. 5. Amplitude of vibratory velocity with varying stiffness k_3.

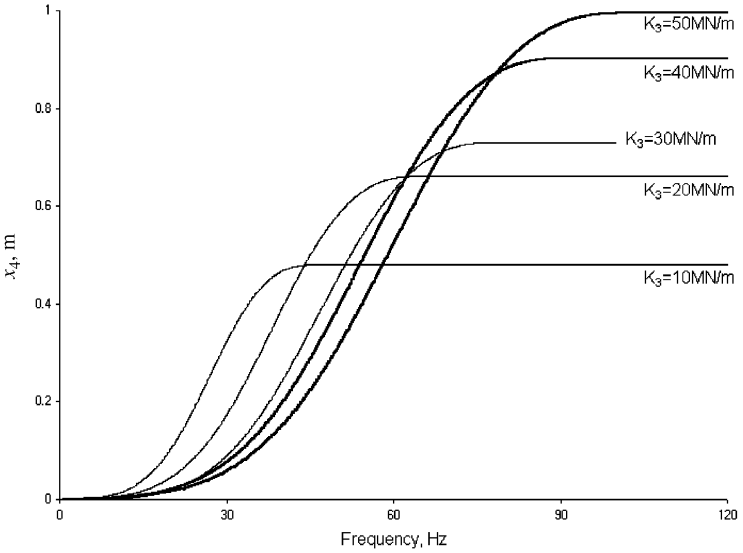

Fig. 6. Displacement of the dry friction element with the varying stiffness k_3.

the dry friction element. It is seen that, for soft medium, the vibration produces a small displacement of the dry friction element.

In soft medium, the energy imparted to the bit is consumed by relatively high amplitude of vibration of the bit. Only a small part of the energy is transferred to the dry friction element and this produces a small displacement. In hard material, the impact produces small deflections but the overall force in the spring and dashpot is large. This force, transmitted to the dry friction element, generates large displacement.

4.2. Study of the system under impact loading

To study the response of the system under successive impacts, a pulse generator is used and the duration of impact is 0.002 s.

From the UCS test, the stiffness of the rock cores was estimated to be 0.9, 1.6 and 2.11 MN/m for the sandstone, limestone and the granite, respectively. The threshold force D was also obtained as 61.9, 140 and 204 kN for the respective types of rock. The core samples and the test complied with the requirements of the ASTM and the British Standard BS1610. The diameter (d) of the cores was 54 mm and the height (L) 108 mm; the ratio L/d is 2 and the standard requires that $2 \leqslant L/d \leqslant 4$. The UCS test was carried out in the civil engineering laboratory of rock mechanics on the "Denison" Block Testing System. A load was applied to each core at the rate of 0.17 kN/s. The computer controlling the testing machine produced the plots of the load against the displacement. The UCS values for the limestone and the granite seem rather higher than average because the rock blocks were of a very good quality, fresh and dry. Consequently, the investigation was carried out within a range covering these values and the following settings were used: $k_3 \in [1,5]$ MN/m, $D \in [50,300]$ kN with a damping ratio $\zeta \in [0.5,1.5]$. These values of the damping ratio allow the observation of the underdamped, critically damped and overdamped motion of the system under impact excitation. Fig. 7 depicts the general motion of the system in time domain, where the dry friction element displays a stepwise displacement.

4.2.1. Underdamped motion

The study of the underdamped motion of the system has been carried out with variation of the stiffness k_3, the damping ratio ζ, the threshold force D, the amplitude and the frequency of impact force. The response of the system has been studied under various combinations of the aforementioned parameters. The aim of this investigation is to estimate the response of different media to the impacting load and the ROP without considering specifics of the tool geometry.

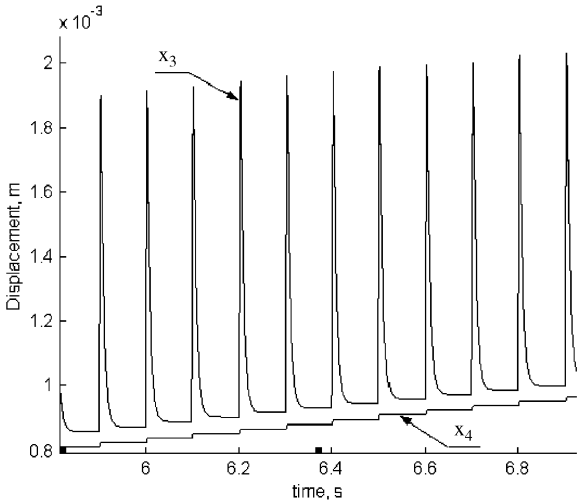

Fig. 7. Typical motion of the system under impact loading.

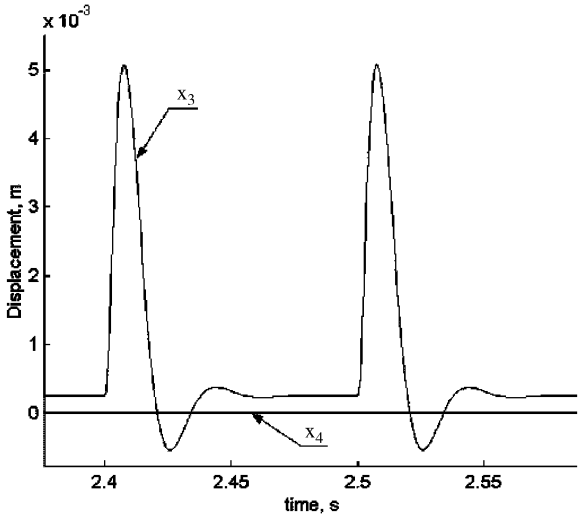

Fig. 8. Response of the system when the medium is very soft; $\zeta = 0.5$.

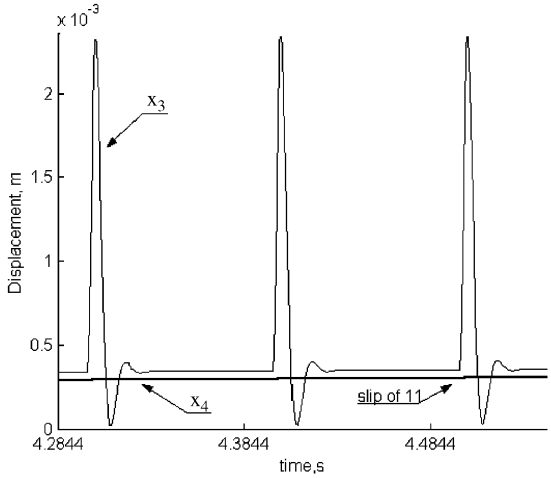

Fig. 9. Bit displacement and initiation of slip of the dry friction element; $\zeta = 0.5$.

Similar to the sweep-sine test in soft medium, all the energy of the impact loading is dissipated by the large deformation of the spring. The energy transmitted to the dry friction element is negligible. This case is shown in Fig. 8, where the displacement (x_3) of bit does not lead to the displacement (x_4) of the dry friction element regardless of the impact force (150–250 kN).

However, for a harder medium slip occurs and Fig. 9 displays the initiation of the slip in the dry friction element. The displacement of the dry friction element is also noticeable in Fig. 7.

To displace the dry friction element 10 in Fig. 2, a static load equal or greater than the threshold force D must be applied. The application of a periodic impact force with very short duration results in an equivalent constant force P, which is the average of the impact force applied over the

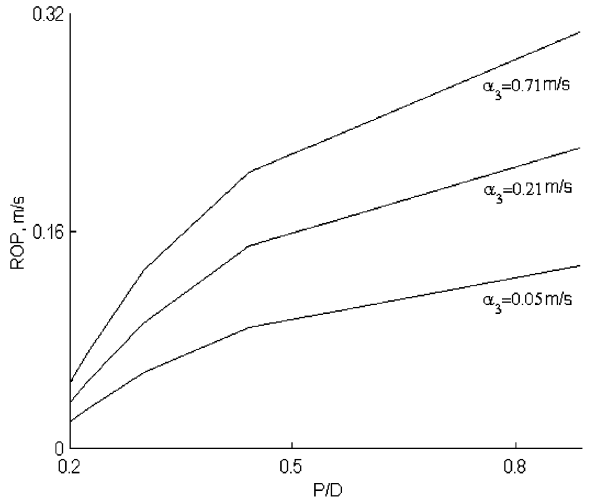

Fig. 10. Relief of the drive for different intensity of vibration; $k_3 = 5\,\mathrm{MN/m}$.

time. The ratio of this constant component P by the threshold force D expresses the dynamic effect of the applied periodic impact force, [17]. The smaller the ratio, the higher is the relief of the thrust, thus the working load is equal to the value of P.

The efficiency of the system can be expressed in terms of the ROP and the overall reduction of the thrust required. It has been noticed that in a soft material, for different values of the vibration velocity α_3, the ROP increases linearly when a relatively small impact force is applied to the system. However, as the stiffness increases or the impact force increases the dependence of the ratio P/D with the ROP becomes non-linear. Fig. 10 displays the efficiency of the vibro-impact process as a plot of the ratio P/D versus the ROP when the applied impact force was equal to 300 kN.

4.2.2. *Overdamped motion of the system*

The study of the overdamped motion of the system is carried out in a similar way to the underdamped. A damping ratio of 1.5 is used and other parameters are varied as described in the above section. It has been observed that for this case, as for the critically damped, the behaviour of the system follows the same pattern as in the underdamped case. Consequently, a similar plot is presented in this section for comparison purposes.

Fig. 11 shows the relationship between the ROP and the force ratio P/D for different vibration intensity when $k_3 = 5\,\mathrm{MN/m}$ and the impact force is 300 kN.

Similar to the above case, it is observed that for a relatively soft media and small impact force, the relationship between the ROP and the relief of the drive varies linearly. As the stiffness and the impact force increase, the relationship becomes non-linear. Figs. 10 and 11 show the relief of the required thrust for different intensities of vibration. It is seen that an average impact load of as much as 20% of the static load will produce a displacement of the dry friction element.

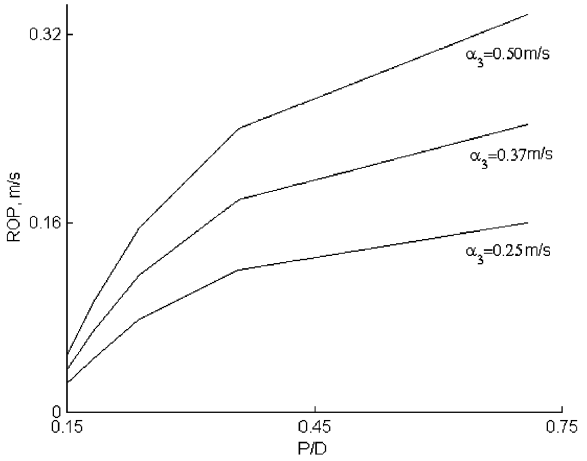

Fig. 11. Relief of the drive for different intensity of vibration; $k_3 = 5\,\mathrm{MN/m}$; $I = 300\,\mathrm{kN}$.

5. Response of the self-oscillatory system

The final system makes use of the model in Fig. 1 as the source of the impact force, which is applied to the model in Fig. 2. The frequency of impact interaction is defined by the stiffness of the springs 3 and 6 (see Fig. 1). The study presented here was carried out with the system frequency equal to 5, 10 and 15 Hz.

Fig. 12 is a screenshot of the simulation process. Fig. 12a displays the bit motion at the top and the motion of the dry friction element underneath. This is in agreement with the aforementioned assumption because the motion of the bit is always positive and this means that the bit is kept constantly in contact with the medium and separation does not occur.

The dry friction element exhibits a stepwise motion where slippage occurs only at the instant of the impact. The dry friction element slips for the duration of the impact and between the intervals of the impacts, it is motionless.

Fig. 12b displays the impact force, the value of which depends on the contact stiffness and the gap between the striker and the bit. A non-Hertzian model of the contact was used assuming that in the contact zone the impacting bodies have visco-elastic properties. This was modelled as a "Kelvin–Voigt" element because this allows the strain and the deformation of the contact layer to develop through the loading and the unloading phases. An instantaneous impact force does not occur thus it is accurately calculated as the force developed during the deflexion of the Kelvin–Voigt element.

Fig. 13 depicts the relationship between the ROP and the force ratio P/D for different stiffness of the medium at an impact frequency of 15 Hz. The simulation showed that higher rates of penetration are produced in hard materials. For increasing stiffness of the medium, the energy of the impact is almost entirely converted into the work of penetration. In a hard material, a small deformation produces large force, which exceeds the threshold force of the material. For a soft medium a part of the imparted energy generates the oscillation of the bit. It should be noted that for a given medium the penetration rate increases with intensity of the vibration activity.

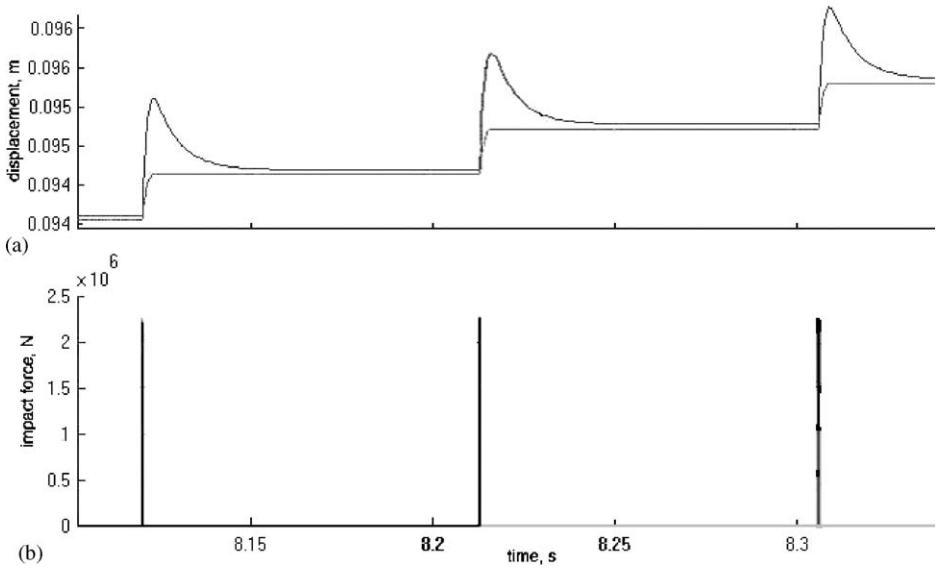

Fig. 12. Screenshot of the simulation process.

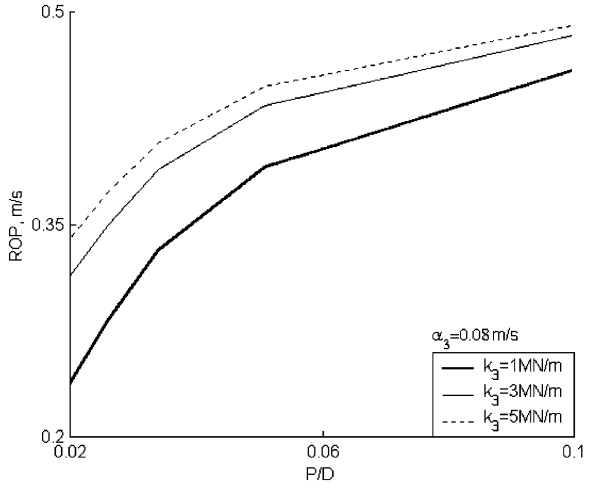

Fig. 13. Relation between the rate of penetration and P/D; $\Omega = 15\,\text{Hz}$.

The phase portrait of the motion of the bit during the penetration process is presented in Fig. 14 and the motion of the striker is shown in Fig. 15. These two plots show that the structure in Fig. 1 has kept its self-sustained periodic performance regardless of the process of penetration. The penetration process is to some extent a perturbation, however this does not affect the stability of the limit cycle.

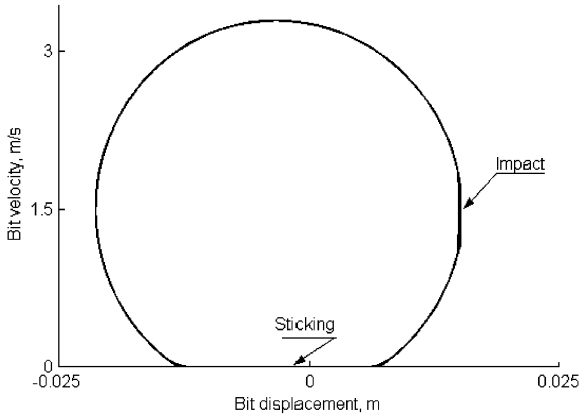

Fig. 14. Phase portrait of bit motion, $\Omega = 10$ Hz.

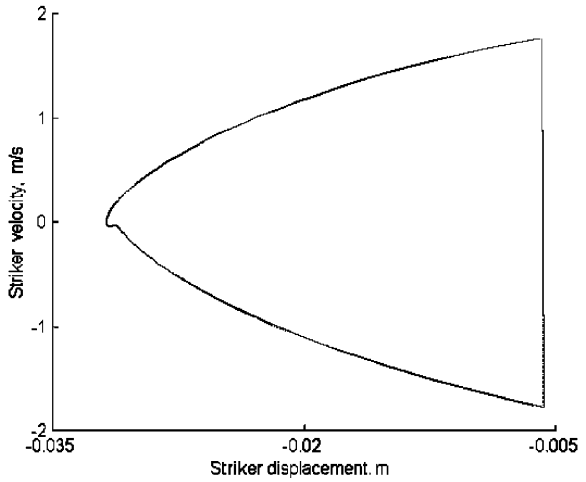

Fig. 15. Phase portrait of striker motion, $\Omega = 15$ Hz.

6. Experimental work

Experimental work has been carried out to study the effect of the application of vibration to conventional rotary drilling. A 72 mm tricone bit is mounted on a shaft, which is driven by an electric motor through a gearbox and a bevel. A strength of materials testing machine is used to apply the required weight on the bit (WOB) and vibration. Fig. 16 is a schematic diagram of the settings of the experiment and Fig. 17 presents the actual view of the experimental rig.

To induce oscillation into the drilling process, a vibration generator incorporated into the system is used together with the servo-hydraulic controller. A weight of 1, 1.5, 2, 2.5 and 3 kN was applied to the drill bit at different speed of rotation. The load on the bit was oscillated sinusoidally at 10 and 15 Hz. The amplitude of oscillation was set to 500 N. Two types of rock were involved in

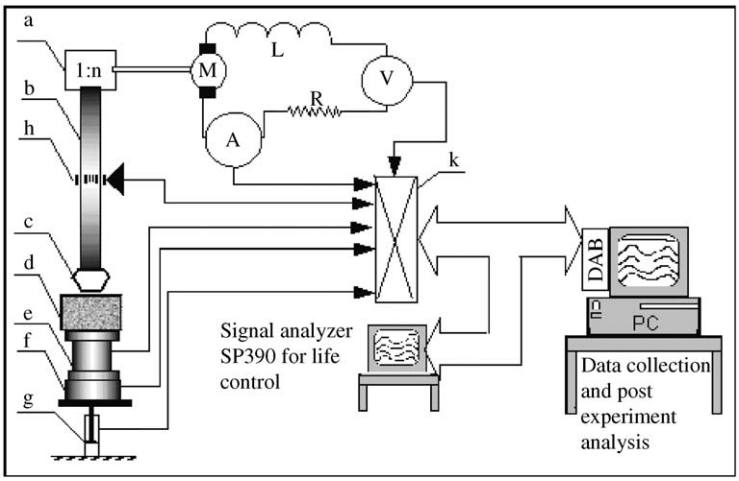

Fig. 16. Schematic diagram of the experimental settings. (a) Gearbox; (b) shaft; (c) drill bit; (d) rock; (e) torque cell; (f) load cell; (g) feed and vibration actuator; (h) speed sensor; (k) connection hub; A, current across motor; V, voltage across motor; L, motor inductance; M, motor rotor; R, motor resistance; DAB, data acquisition board.

Fig. 17. A view of the experimental rig.

this experiment, namely limestone and sandstone. The aim of this preliminary test drilling is to determine the initial improvement of the ROP by superimposing vibration. Thus, this experiment does not carry any optimization process.

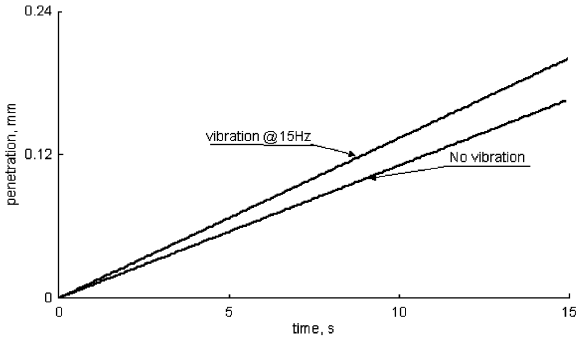

Fig. 18. Drilling in sandstone, WOB 1.5 kN at 50 rpm.

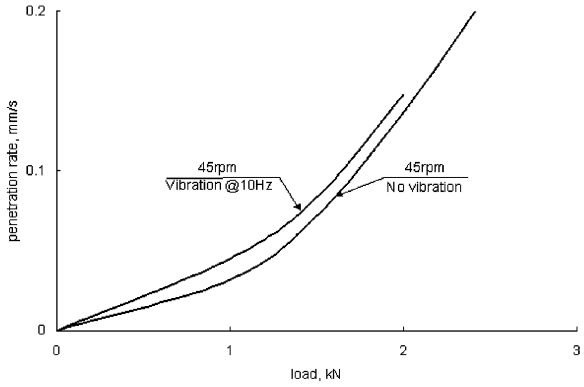

Fig. 19. Rate of penetration in sandstone.

Fig. 18 shows the average rate of drilling in sandstone obtained from the linear regression of the actual signal. A weight of 1.5 kN was applied to the bit at a rotational speed of 50 rpm. The frequency of the superimposed vibration was 15 Hz and the amplitude was 500 N. The analysis shows that for the same parameters of the system configuration, drilling with superimposed vibration produced higher ROP. With reference to Fig. 18, the system drilled 1.2 times faster with superimposed vibration than with conventional drilling.

To estimate the impact of the application of vibration to the drilling process, the ROP is presented as a function of the load (weight) on the bit. Fig. 19 shows this dependence for the sandstone. The speed of rotation was 45 rpm and the relationship between the rates of drilling with and without vibration shows an increase of 8–10% on the linear portion of the curves.

Fig. 20 displays the same trend when drilling in the limestone blocks. Here the ROP obtained at 80 rpm is compared to the penetration when the rotation speed is 45 rpm with applied vibration at 15 Hz. The linear sections of the curves show that with vibration the system drills 1.5 times faster than conventional drilling, although the speed of rotation is considerably smaller.

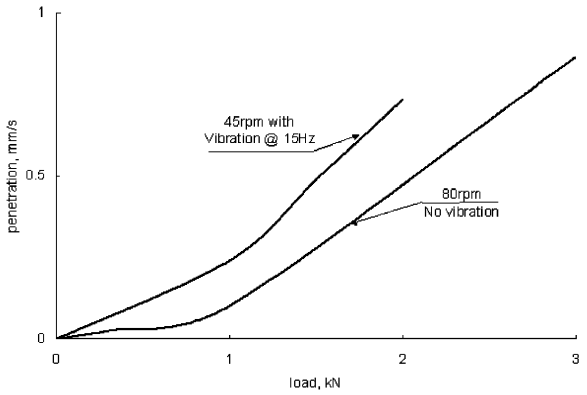

Fig. 20. Rate of penetration in limestone.

7. Conclusion

The model of impact penetration into hard media presented in this paper continues the study of the self-oscillatory system for percussive-rotary drilling presented in Ref. [1]. The results show that it is possible to obtain considerable reduction of the thrust required. The relief of the thrust is expressed by the force ratio P/D and the smaller this ratio is, the higher is the effect of the applied vibration. The impact load produces not only fast penetration but it also weakens the upper layer of the medium underneath due to propagation of cracks. This eases the rotary process because the cutting will occur in a pre-fragmented medium. It is assumed that the impact loading does not affect the rotational motion of the bit because a stable steady motion has been obtained in Ref. [1] under this effect.

The preliminary test drilling shows that the application of vibration to the drilling process brings a remarkable increase in the ROP. This result supports the concept of percussive-rotary drilling. It shows that even at 10–15 Hz the superimposed vibration brings a significant increase in the ROP.

The results obtained show that the structure presented has a stable regime of operation for realistic parameters. The mathematical tool developed allows the optimal parameters of the system to be defined. This and the accumulated theoretical knowledge can provide design criteria for new vibro-impact drilling systems to accommodate the presented structure. A successful implementation will provide the drilling industry with an advanced technique, which will protect the drill string from hazardous vibration, adjust itself to the drilling conditions, and increase the performance of the drilling tools.

References

[1] D.R. Pavone, Application of high sampling rate downhole measurements for analysis and cure of stick–slip, SPE 28324, 1994.

[2] A.D. Batako, V.I. Babitsky, N.A. Halliwell, Self-excited system of percussive-rotary drilling, *Journal of Sound and Vibration* 259 (1) (2003) 97–118.

[3] S.A. Tsaplin, Vibro-impact Mechanisms for Road and Bridge Construction, National Engineering Laboratory Translation No. 1003, Autotransizdat, Moscow, 1953 (in Russian).
[4] D.D. Barkan, *Vibro-method in Civil Engineering*, Gossizdat, Moscow, 1959 (in Russian).
[5] O.A. Savinov, A.Ya. Luskin, *Vibration Method of Pile Driving and its Application in Civil Engineering*, Gossizdat, Moscow, 1960 (in Russian).
[6] B.M. Rebrik, *Drilling During the Engineering-Geological Exploration*, Nedra, Moscow, 1979 (in Russian).
[7] G.G. Azbel, O.A. Savinov, M.G. Tseitlin, Vibratory machines for pile driving and geological drilling, in: E.E. Lavendel (Ed.), *Vibration Processes and Machines, Vibration in Engineering,* Vol. 4, Machinostroenie, Moscow, 1981, pp. 325–335 (in Russian).
[8] M.G. Tseitlin, V.V. Verstov, G.G. Azbel, *Vibration Engineering in Pile Driving and Drilling*, Stroyizdat, Leningrad, 1987 (in Russian).
[9] V.I. Babitsky, Theory of Vibro-impact Systems and Applications, Springer, Berlin, Revised translation from Russian, Moscow, Nauka, 1978.
[10] Yu.I. Neimark, Theory of vibration driving and vibro-penetration, in: Engineering Collection, Vol. 16, Academy of Science, Moscow, 1953 (in Russian).
[11] I.I. Blekhman, Investigation of the process of vibration driving of plies, in: Engineering Collection, Vol. 19, Academy of Science, Moscow, 1954 (in Russian).
[12] I.I. Blekhman, Vibrational Mechanics, World Scientific, Singapore. Translation from Russian, Moscow, VO Nauka, 1994, 1999 (in Russian).
[13] M. Spektor, Principle of soil-tool interaction, *Journal of Terramechanics* 18 (1) (1981) 51–65.
[14] M. Spektor, Motion of soil-working tool under impact loading, *Journal of Terramechanics* 18 (3) (1981) 133–156.
[15] M. Spektor, Working processes of cyclic-action machinery for soil deformation—Part I, *Journal of Terramechanics* 20 (1) (1983) 13–41.
[16] R.D. Neilson, A.A. Odger, R.G. Stevenson, Development of a computer based model of vibro-impact driving, *Machine Vibration* 3 (1995) 164–175.
[17] V.K. Astahev, V.I. Babitsky, M.Z. Kolovsky, *Dynamics and Control of Machines*, Springer, Berlin, 2000.